

# Modelling the spectral energy distribution of galaxies from the ultraviolet to submillimeter

Cristina C. Popescu<sup>1,2,3</sup> and Richard J. Tuffs<sup>4</sup>

<sup>1</sup> The Observatories of the Carnegie Institution of Washington,  
813 Santa Barbara Str., Pasadena, CA 91101, USA,  
popescu@ociw.edu

<sup>4</sup> Max Planck Institut für Kernphysik, Saupfercheckweg 1,  
69117 Heidelberg, Germany

## Abstract

*We present results from a new modelling technique which can account for the observed optical/NIR - FIR/submm spectral energy distributions (SEDs) of normal star-forming galaxies in terms of a minimum number of essential parameters specifying the star-formation history and geometrical distribution of stars and dust. The model utilises resolved optical/NIR images to constrain the old stellar population and associated dust, and geometry-sensitive colour information in the FIR/submm to constrain the spatial distributions of young stars and associated dust. It is successfully applied to the edge-on spirals NGC 891 and NGC 5907. In both cases the young stellar population powers the bulk of the FIR/submm emission. The model also accounts for the observed surface brightness distribution and large-scale radial brightness profiles in NGC 891 as determined using the Infrared Space Observatory (ISO) at 170 & 200  $\mu\text{m}$  and at 850  $\mu\text{m}$  using SCUBA.*

## 1 Introduction

Historically, almost all our information about the current and past star-formation properties of galaxies has been based upon spatially integrated measurements in the ultraviolet (UV), visible and near-infrared (NIR) spectral regimes. However, star-forming galaxies contain dust which absorbs some fraction of the emitted starlight, re-radiating it predominantly in the far-infrared (FIR)/sub-millimeter(submm) range. The true significance of this process even for “normal” (i.e. non-starburst) galaxies has been revealed by observations of a representative sample of late-type Virgo cluster galaxies with the ISOPHOT instrument on board the Infrared Space Observatory (ISO). These showed the dust emission to typically account for 50 percent of the bolometric output of these systems, with a spectral peak generally lying between 100 and 250  $\mu\text{m}$  (Tuffs et al. 2002; Popescu et al. 2002).

---

<sup>2</sup>Otto Hahn Fellow of the Max Planck Institut für Astronomie, Königstuhl 17, 69117 Heidelberg, Germany

<sup>3</sup>Research Associate, The Astronomical Institute of the Romanian Academy, Str. Cuțitul de Argint 5, Bucharest, Romania

In view of this, the measurement of current and past star-formation in galaxies - and indeed of the universe as a whole - requires a quantitative understanding of the role different stellar populations play in powering the FIR/submm emission. For this both optical and FIR/submm data needs to be used, as they contain complementary information about the distribution of stars and dust.

On the one hand, optical data probes the colour and spatial distribution (after correction for extinction) of the photospheric emission along sufficiently transparent lines of sight. This is particularly useful to investigate older, redder stellar populations in galaxian disks with scale heights larger than that of the dust. On the other hand, grains act as test particles probing the strength and colour of ultraviolet (UV)/optical interstellar radiation fields. This constitutes an entirely complementary constraint to studies of photospheric emission. In the FIR, grains are moreover detectable over almost the full range of optical depths present in a galaxy. At least part of this regime is inaccessible to direct probes of starlight, especially at shorter wavelengths, even for face-on systems. This particularly applies to light from young stars located in, or close by, the dust clouds from which they formed, since a certain fraction of the light is locally absorbed. Furthermore, there is at least a possibility that most of the remaining UV and even blue light from young stars that can escape into the disk might be absorbed by diffuse dust there. A combined analysis of the whole UV-optical/FIR/submm spectral energy distribution (SED) of galaxies seems to be a promising way to constrain the problem.

Here we present the results from a new tool for modelling the optical-FIR/submm SED of galaxies (Popescu et al. 2000b, Misiriotis et al. 2001). Our model predicts the SED as a function of intrinsic SFR, star formation history (from population synthesis calculations) and dust content. This tool includes solving the radiative-transfer problem for a realistic distribution of absorbers and emitters, considering realistic models for dust (taking into account the grain-size distribution and stochastic heating of small grains) and the contribution of HII regions. The model addresses the fundamental and controversial question of optical thickness in the disk of galaxies and can account for the detailed UV-optical-FIR-submm SED with an absolute minimum of independent physical variables, each strongly constrained by data.

## 2 An overview of SED modelling in the literature

The SED models of galaxies have been built using the tools and results from previous studies of the key ingredients required by such models: radiative transfer codes and dust emission models. Radiative transfer codes were initially developed to account for the UV-optical/NIR appearance of galaxies, their extinction properties, and the role the spatial distribution of stars and dust play in shaping the SED. These codes used either analytical methods

(Kylafis & Bahcall (1987) or Monte Carlo simulations (Witt & Gordon 1996, 2000, Ferrara et al. 1999, Gordon et al. 2001). In parallel, dust models have been built to model extinction curves and the heating and emission of grains in different environments. These include the studies of Mathis et al. (1977), Draine & Lee (1984), Draine & Anderson (1985), Dwek (1986), Guhathakurta & Draine (1989), Désert et al. (1990), Laor & Draine (1993), Weingartner & Draine (2001).

Applications of such methods to study the SED of galaxies have been initiated, as expected, in the optical/NIR regime. Thus, in their fundamental work, Kylafis & Bahcall (1987) applied a radiation transfer modelling technique to edge-on systems, where the scale height of the stars and dust extinction can be directly constrained. The technique was subsequently applied on several edge-on galaxies by Xilouris et al. (1997, 1998, 1999). Radiative transfer codes in combination with observations of nearby edge-on galaxies were also used by Ohta & Kodaira (1995), Kuchinski et al. (1998) and Matthews & Wood (2001).

A further step in the SED modelling was to include the FIR-submm spectral regime in the overall analysis. Different tools have been proposed starting with the pioneering works of Xu & Buat (1995) and Xu & Helou (1996). They used radiative transfer codes for an assumed “sandwich” configuration of dust and stars and considered in detail the relative contribution of the non-ionising UV photons and the optical photons in heating the grains. However, these calculations did not incorporate a model for the dust grain emission, nor for radial variations in the absorbed radiation in the disk, and therefore could not account for the shape of the FIR SED.

Recently, there have been several works modelling the SED of galaxies from the UV to submm, which considered more realistic geometries and dust models, and which have started to make use of the new observational data becoming available at longer FIR/submm wavelengths. In parallel with these self-consistent models a series of empirical or semi-empirical approaches for modelling the SED from UV to submm wavelengths have been adopted, mainly for statistical applications (Devriendt et al. 1999, Dale et al. 2001).

Self consistent calculations of the SED over the entire spectral range have been developed slowly, due to the large amount of computational time required both for the radiative transfer and for the calculation of the probability distribution of temperatures of dust grains, especially of the small grains, which undergo large temperature fluctuations. To this should be added that it is only now becoming possible to obtain resolved images covering the MIR to FIR and submm spectral range, even for nearby galaxies. Such observations are needed for constraining SED models. Recent self-consistent SED modelling was presented by Silva et al. (1998). They applied photometric and chemical evolution models of galaxies to explain the SED of both normal and starburst galaxies. Their model considers radiative transfer in both the molecular clouds and in the diffuse ISM, and includes a consistent treatment of dust emission and stochastic heating of small grains. It can thus reproduce reasonably well the SED of the studied galaxies, in both the optical and FIR spectral range

and is therefore suited to describe the general shape of the volume-integrated SED. The model has however more free parameters than the generally available observational constraints and the solution obtained may not be unique. The model is also less adequate in describing the intrinsic distributions of stars and dust because of its simplified geometry. For example the model does not consider different scale heights and scale lengths for the stellar and dust distribution. Furthermore, all stellar populations are constrained to have the same scale heights, including the young stellar population which is known to reside in a very thin stellar disk. The radiative transfer is only an approximation, and is rigorously applicable only to an infinite homogeneous medium, and there is no treatment of anisotropic scattering.

Bianchi et al. (2000) attempted to model NGC 6946 from the UV to FIR using a 3D Monte Carlo radiative-transfer code for a simplified geometry of emitters (a single stellar disk). They concluded that the total FIR output is consistent with an optically thick solution. This result should be considered with caution as their model makes a number of simplifications. For example they did not consider a size distribution for grains and there is no consistent treatment of grain heating and emission. Accordingly, there is no calculation of stochastic heating for small grains, but rather a MIR correction calculated according to the model of Désert et al. (1990). Furthermore the model did not consider the contribution of localised sources within star-forming complexes. This resulted in a poor fit of the FIR SED and a failure to reproduce the IRAS flux densities.

Several studies have been dedicated to modelling the SED of starburst galaxies. Recent work on modelling the UV to submm emission was presented by Efstathiou et al. (2000) for starburst galaxies, which were treated as an ensemble of optically thick giant molecular clouds (GMCs) centrally illuminated by recently formed stars. The model has a proper treatment of dust emission, including stochastic heating of small grains, and it allows for the star-forming complexes to evolve with time, based on a physical model of the dusty HII region phase and of the supernova phase. The star-forming complexes are modelled assuming spherical symmetry, which, as remarked by the authors, may not be true in the later stages of the GMC evolution. Also there is no further transfer of radiation between GMCs, meaning that the stellar light is not allowed to escape the GMC. The FIR spectrum is fitted for an exponential decaying star formation rate, where the age and time constant of the star-burst (or in some cases of two star-bursts) are fitted parameters. This modelling technique successfully reproduced the observed SED of M 82 and NGC 6090, though for the latter case there is an ambiguity between the existence of an older burst and a diffuse component not considered in the model. Obviously this method is suitable for starburst dominated galaxies and can bring interesting insights into the ages of the stellar populations, but cannot be applied to normal “quiescent” disk galaxies dominated by emission from the diffuse interstellar radiation field.

Bekki et al. (2000) studied the time evolution of the SED in starburst galaxies based on numerical simulations that can analyse simultaneously dy-

namical and chemical evolution, structural and kinematical properties. This method is rather unique and can be used to study mergers, for example, or other physical processes related to galaxy formation. The price to pay for this complexity is the quite rudimentary treatment of the radiative transfer and dust emission: scattering has been neglected from the radiative transfer, there is no grain size distribution and no treatment of stochastic heating of small grains. Therefore, their model can be used to indicate trends in the SED evolution rather than to give quantitative predictions and is suitable for numerical simulations.

As a general remark, most of the work described above has been concentrated in fitting the volume-integrated emission of the galaxies at different spectral wavelengths and has not been constrained by morphological information from images. A more robust knowledge of the intrinsic distributions of stellar populations and dust, and ultimately of the SF history in galaxies can be gained if also the surface brightness distribution of optical and even FIR emission can be analysed. The method we present here constrains the problem by using the whole information in the brightness distribution. This approach has been only used in the optical/NIR regime, by Xilouris et al. (1997, 1998, 1999). With the ISO and SCUBA data we are now able to make predictions also for the appearance of the FIR/submm images and compare the predicted maps with the observed ones. In the future SIRTf observations will extend knowledge of the FIR morphology in galaxies and will bring new constraints for the SED modelling methods.

### 3 Our model

Star-forming galaxies are fundamentally inhomogeneous, containing highly obscured massive star-formation regions, as well as more extended structures harbouring older stellar populations which may be transparent or have intermediate optical depths to starlight. Accordingly, our model divides the stellar population into an “old” component (considered to dominate the output in B-band and longer wavelengths) and a “young” component (considered to dominate the output in the non-ionising UV).

#### 3.1 The “old” stellar population

The “old” stellar population is generally observed to have scale heights of several hundred pc in rotationally supported spiral galaxies, a result which can be physically attributed to the increase of the kinetic temperature of stellar populations on timescales of order Gyr due to encounters with molecular clouds and/or spiral density waves. This means that the “old” stellar population can be constrained from resolved optical and near-IR images via the modelling procedure of Xilouris et al. (1999). The procedure uses the technique for solving the radiation transfer equation for direct and multiply scattered light for arbitrary geometries by Kylafis & Bachall (1987).

For edge-on systems these calculations completely determine the scale heights and lengths of exponential disk representations of the old stars (the “old stellar disk”) and associated diffuse dust (the “old dust disk”), as well as a dustless stellar bulge. This process is feasible for edge-on systems since the scale height of the dust is less than that of the stars. For face-on systems the scale height cannot be fixed by the optical data alone, and must be determined through consideration of its effect on the FIR SED.

The extinction law of the dust can be directly determined from the observed optical/near-IR wavelength, since the calculation is done independently at each wavelength. In all cases so far, an extinction law consistent with that predicted from the graphite/silicate mix of Laor & Draine (1993) and the  $a^{-3.5}$  grain size distribution of Mathis Rumpl & Nordsieck (1977) has been found (Xilouris et al. 1999).

### 3.2 The “young” stellar population

The “young” stellar population is also specified by an exponential disk, which we shall refer to as the “young stellar disk”. Invisible in edge-on systems, its scale height is constrained to be 90 pc (the value for the Milky Way) and its scale length is equated to that of the “old stellar disk” in B-band. The emissivity of the “young stellar disk” is parameterised in terms of the current star formation rate ( $SFR$ ) by relating the non-ionising UV emission to  $SFR$  using the population synthesis models of Bruzual & Charlot (2001) for  $Z = Z_{\odot}$ , a Salpeter initial mass function, a mass cut-off of  $100 M_{\odot}$ , and an exponential decrease of the  $SFR$  with time, with a time constant  $\tau = 5 Gyr$ .

A second exponential dust disk of grain mass  $M_{dust}$  - the “second dust disk” is associated with the young stellar population. This is needed to account for the observed submm emission from edge-on disk galaxies, which cannot be reproduced by models containing only the old dust disk determined from the optical images (Popescu et al. 2000b, Misoritis et al. 2001). It is constrained to have the same scale length and height as that of the young stellar disk. This second dust disk is assumed to be composed of grains with the same graphite/silicate and  $a^{-3.5}$  grain size distribution as for the old dust disk. All the exponential disks for young and old stars and dust in the model are truncated at three times the exponential scale length. Because two disks of dust are required for the model, we refer to it as to the “two-dust-disk” model.

The current star-formation rate ( $SFR$ ) and mass of the second dust disk ( $M_{dust}$ ) are the first two primary free parameters of the model to determine the FIR/submm radiation. They both relate to the smooth distribution of stars and dust in the second disk. A third primary parameter,  $F$ , is included to account for inhomogeneities in the distributions of dust and stars in the young stellar disk.  $F$  is defined as the fraction of non-ionising UV which is locally absorbed in HII regions around the massive stars. It determines the additional likelihood of absorption of non-ionising UV photons due to autocorrelations between an inhomogeneous distribution of young stars and parent molecular clouds. Astrophysically, this arises because at any particular

epoch some fraction of the massive stars have not had time to escape the vicinity of their parent molecular clouds. Thus,  $F$  is related to the ratio between the distance a star travels in its lifetime due to its random velocity and the typical dimensions of star-formation complexes.

### 3.3 Calculation of dust emission

The first step in the calculation of the dust emission is to determine the radiation energy density of the unabsorbed light versus wavelength from the non-ionising UV to the near-IR for the diffuse radiation field. This is done for trial values of the mass of dust in the second dust disk  $M_D$  by solving the radiation transfer equation for the observed optical wavelengths and three wavelengths in the non-ionising UV. (For edge on systems,  $M_D$  is independent of the dust mass in the old dust disk, which is fixed by the optical observations). The actual energy density distribution can then be determined for any trial combination of  $SFR$  and  $F$  without a further radiation transfer calculation. Both the colour and intensity of the radiation field vary with position in different ways according to the combination of  $SFR$ ,  $M_D$  and  $F$ .

The FIR/submm emission for each combination of  $SFR$ ,  $M_D$  and  $F$  is then calculated for graphite and silicate grains of size  $a$  immersed in the radiation field at each point of a grid of positions in the galaxy, including an explicit treatment of stochastic emission. Subsequently we integrate over the entire galaxy to obtain the FIR-submm SED of the diffuse disk emission. Prior to comparison with observed FIR-submm SEDs, an empirically determined spectral template for the HII regions, scaled according to the value of  $F$ , must be added to this calculated spectral distribution of diffuse FIR emission.

Due to the precise constraints on the distribution of stellar emissivity in the optical-NIR and the distribution and opacity of dust in the “old dust disk” yielded by the radiation transfer analysis of the highly resolved optical-NIR images, coupled with the simple assumptions for the distribution of the young stellar population and associated dust, our model has just three free parameters -  $SFR$ ,  $F$  and  $M_{\text{dust}}$ . These fully determine the FIR-submm SED, and allow a meaningful comparison with broad-band observational data in the FIR/submm, where, in particular for distant objects, typically only a few spectral sample points for the spatially integrated emission are available. The parameters are strongly coupled, but in general terms,  $M_{\text{dust}}$  is principally constrained by the submm emission,  $SFR \times (1 - F)$  by the bolometric FIR-submm output and the factor  $F$  (in the absence of high resolution images and/or for edge-on systems) by the FIR colour.

## 4 Application to edge-on spiral galaxies

Modelling edge-on spiral galaxies has several advantages, mainly when investigating them in the optical band. One advantage is that, in this view of a galaxy, one can easily separate the three main components of the galaxy

(i.e., the stellar disk, the dust and the bulge). Another advantage is that the dust is very prominently seen in the dust lane, and thus its scalelength and scaleheight can be better constrained. A third advantage is that many details of a galaxy that are evident when the galaxy is seen face-on (e.g., spiral arms), are smeared out to a large degree when the galaxy is seen edge-on (Misiriotis et al. 2000). Thus, a simple model with relatively few parameters can be used for the distribution of stars and dust in the galaxy. However, in edge-on galaxies it is very difficult to see localised sources (i.e., HII regions), in which the radiation can be locally absorbed and thus not contribute to the diffuse radiation field. Also, if the galaxy has a thin (young) stellar/dust disk, highly obscured by the dust lane in the plane of the galaxy, then this disk cannot be inferred from observations in the optical/NIR spectral range. As described in the previous section, our model makes use of the information in the FIR-submm regime to constrain this problem.

We first applied the above method to the well-known edge-on spiral galaxy NGC 891. This is one of the most extensively observed edge-on galaxies in the nearby universe, which makes it ideal for a verification of our modelling technique. We have also extended our SED modelling technique to four additional edge-on systems - NGC 5907, NGC 4013, UGC 1082 and UGC 2048 - with the aim of examining whether the features of the solution we obtained for NGC 891 might be more generally applicable. In this section we mainly show and discuss the results for NGC 891, and only briefly illustrate the solution for NGC 5907.

The “two-dust-disk” model can successfully fit the shape of the SED for both NGC 891 and NGC 5907. The best solution for NGC 891 (Fig. 1) has a central face-on V-band optical thickness  $\tau_V^f = 3.1$  and a corresponding non-ionising UV luminosity  $\sim 8.2 \times 10^{36}$  W. The luminosity of the diffuse component is  $4.07 \times 10^{36}$  W, which accounts for 69% of the observed FIR luminosity, and the luminosity of the HII component is  $1.82 \times 10^{36}$  W, making up the remaining 31% of the FIR luminosity. The best solution for NGC 5907 (Fig. 2) has a central face-on optical depth in the optical band  $\tau_V = 1.4$ . The total FIR-submm re-radiated luminosity of NGC 5907, obtained by integrating the “two-dust-disk” model SED, is  $50.5 \times 10^{35}$  W out of which  $27.0 \times 10^{35}$  W is attributed to heating from the young stellar population. Thus, about 40% of the dust emission is powered by the old stellar population. The major difference between NGC 891 and NGC 5907, on the basis of the “two-dust-disk” model, is that the spectrum of the former apparently allows for the existence of a larger contribution from HII regions (see Misiriotis et al. 2001 for a detailed discussion) -  $F$  takes values of 0.22 and 0.10, respectively. Such small values of  $F$  are expected for “normal” galaxies, in contrast to starburst systems, where the FIR/submm SEDs peak shortwards of  $100 \mu\text{m}$ , and one would anticipate that  $F$  would be closer to unity.

In both cases most of the luminosity comes from the diffuse component, and the main heating source is provided by the young stellar population. The relative contribution of optical and UV photons in heating the dust has been a longstanding question in the literature. Since we have a detailed calculation



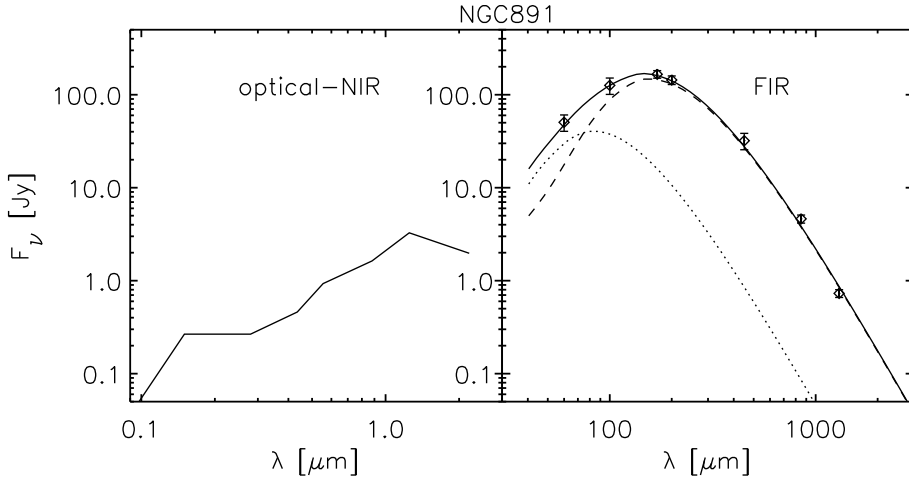


Figure 1: The predicted SED of NGC 891 from the “two-dust-disk” model with  $SFR = 3.8 M_{\odot}/\text{yr}$ ,  $F = 0.22$  and  $M_{\text{dust}} = 7 \times 10^7 M_{\odot}$  in the second disk of dust. LH panel: the intrinsic emitted stellar radiation (as would have been observed in the absence of dust). RH panel: the re-radiated dust emission, with diffuse and HII components plotted as dashed and dotted lines, respectively. The data (integrated over  $\pm 225''$  in longitude), are from Alton et. al 1998 (at 60, 100, 450 & 850  $\mu\text{m}$ ), Guélin et al. 1993 (at 1300  $\mu\text{m}$ ) and from Popescu et al. (2001) (at 170 & 200  $\mu\text{m}$ ).

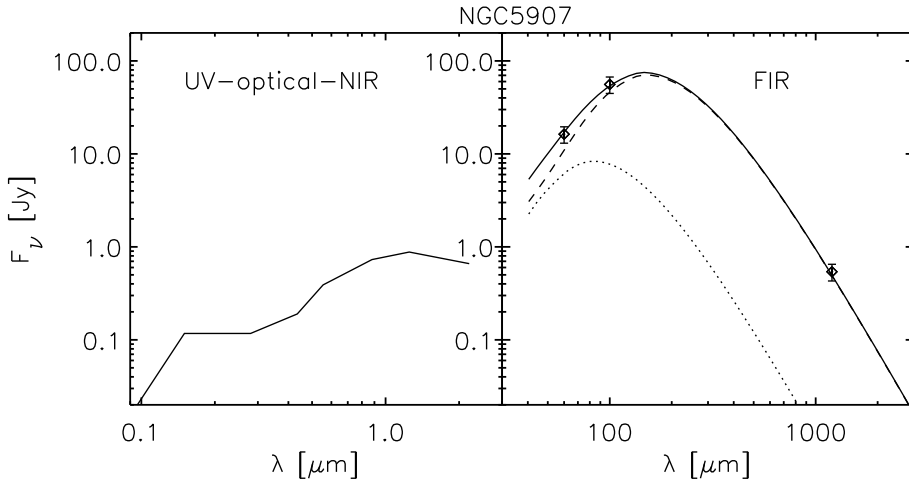


Figure 2: The predicted SED of NGC 5907 from the “two-dust-disk” model with  $SFR = 2.2 M_{\odot}/\text{yr}$ ,  $F = 0.10$  and  $M_{\text{dust}} = 4.5 \times 10^7 M_{\odot}$  in the second disk of dust. The legend is as in Fig. 1. The data are from Young et al. (1989) (at 60 & 100  $\mu\text{m}$ ), and from Dumke et al. (1997) (at 1200  $\mu\text{m}$ )

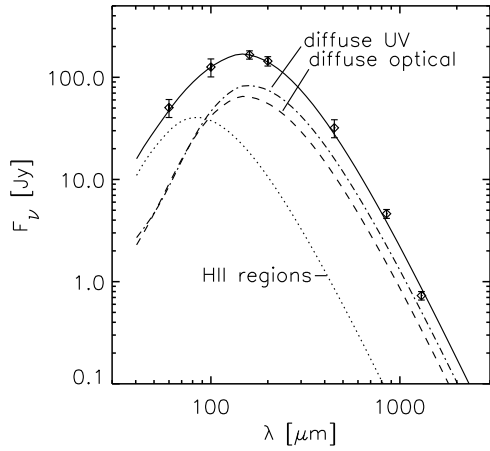


Figure 3: The absolute contribution of the three stellar components to the FIR emission versus wavelength for the “two-dust-disk” model. Dashed-line: diffuse optical radiation (4000 – 22000 Å); dashed-dotted line: diffuse UV radiation (912 – 4000 Å); dotted-line: HII regions. The total predicted FIR SED is given by the solid line. The data points are as for Fig. 1.

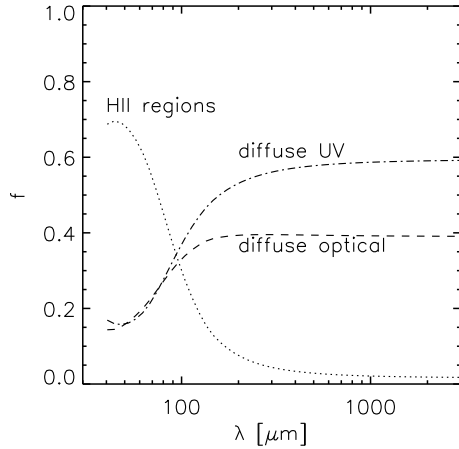


Figure 4: The fractional contribution of the three stellar components to the FIR emission versus wavelength for the “two-dust-disk” model. The legend is as for Fig. 3 and the data points are as for Fig. 1.

of the absorbed energy over the whole spectral range and at each position in the galaxy, we can directly calculate which part of the emitted FIR luminosity from each volume element of the galaxy is due to the optical and NIR photons, and which part is due to the UV photons. In this way we can also predict the contribution of different stellar populations in heating the dust as a function of FIR wavelength. Volume-integrated IR spectral components

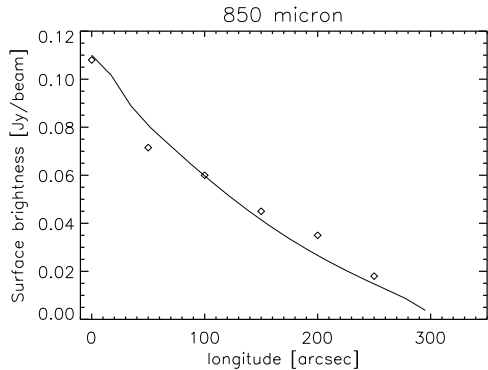


Figure 5: The averaged radial profile of NGC 891 at  $850\ \mu\text{m}$  from the diffuse component of the “two-dust-disk” model, plotted with the solid line. The profile is averaged over a bin width of  $36''$ , for a sampling of  $3''$  and for a beam width of  $16''$ , in the same way as the observed averaged radial profile from Alton et al. (2000) (plotted with diamonds).

arising from re-radiated optical and UV light are presented in Figs. 3,4 for the case of NGC 891. We note that the diffuse optical radiation field makes only a relatively small contribution to the total emitted dust luminosity. This is in qualitative agreement with various statistical inferences linking FIR emission with young stellar populations, in particular the FIR-radio correlation. Our analysis predicts the predominance of UV-powered grain emission even in the submm range, which, in turn, would predict a tighter FIR-radio correlation when the FIR luminosity integrated over the FIR-submm range is considered. This prediction has been recently confirmed by Popescu et al. (2002), using the new ISOPHOT observations of a complete sample of late-type Virgo cluster galaxies (Tuffs et al. 2002).

A more stringent test of the model is to compare its predictions for the morphology of the dust emission with spatially resolved maps. Because observed radial profiles were derived by Alton et al. (2000) using the SCUBA observations at  $850\ \mu\text{m}$ , we first attempt to calculate the radial profiles at this wavelength and compare it with the observations (Fig. 5), which are mainly sensitive to dust column density. We have found that in the case of the “two-dust-disk” model there is a very good agreement between the model predictions and the observations, where the observed profiles were mirrored for compatibility with the symmetry in our model. The predicted radial profile can be traced out to 300 arcsec radius (15 kpc), as also detected by the SCUBA.

Recent deep observations of NGC 891 with the ISOPHOT instrument at 170 and  $200\ \mu\text{m}$  (Popescu et al. 2001) offer a still stronger test of the model, as the FIR emission here depends on the distribution of both stellar luminosity and dust.

Simulated FIR maps were obtained using the actual pointing data to scan

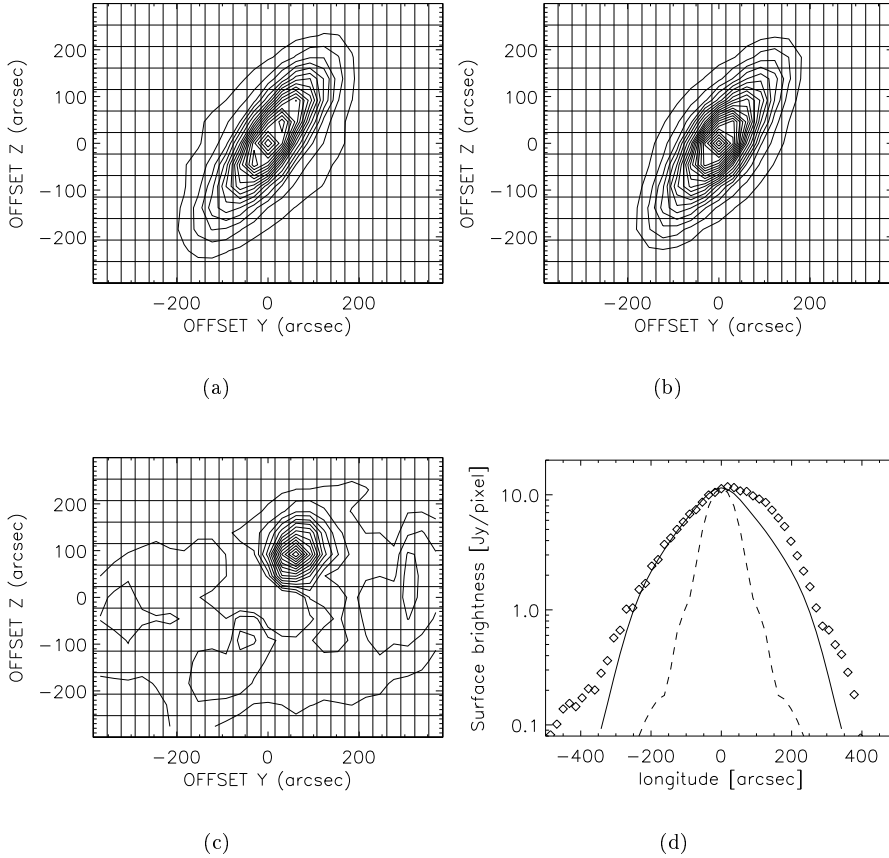


Figure 6: a) Contour plot of the observed brightness distribution at  $170\ \mu\text{m}$ . The contours are plotted from  $10.7$  to  $230.0\ \text{MJy/sr}$  in steps of  $12.2\ \text{MJy/sr}$ . The grid indicates the actual measured sky positions sampled at  $31 \times 46$  arcsec in the spacecraft coordinates Y and Z. b) Contour plot of the simulated diffuse brightness distribution at  $170\ \mu\text{m}$ . The contours are plotted from  $10.4$  to  $239.7\ \text{MJy/sr}$  in steps of  $10.4\ \text{MJy/sr}$ . c) Contour plot of the observed minus simulated diffuse brightness distribution at  $170\ \mu\text{m}$ . The contours are plotted from  $2.2$  to  $46.1\ \text{MJy/sr}$  in steps of  $3.1\ \text{MJy/sr}$ . The unresolved source from the Northern side of the galaxy and the faint extended source from the Southern side account for  $8\%$  of the total integrated flux density, in agreement with our model prediction for the FIR localised sources at this wavelength. d) The longitudinal profile (diamonds) observed by ISO at  $170\ \mu\text{m}$  (Popescu et al. 2001), with a common bin width and sampling interval of  $18.4''$ . North is towards positive longitude. The solid line is the prediction from the diffuse component of the “two-dust-disk” model and the dashed line the projected beam profile (FWHM  $1.8\ \text{arcmin}$ .)

the diffuse disk model. The model map was then convolved with empirical PSFs derived from point source measurements. The comparison between the observed map (Fig. 6a) and the simulated one (Fig. 6b) show a remarkable agreement. To search for small differences between the model and the observations, not detectable in the maps due to the high dynamical range of the displayed data, we present in Fig. 6c the residual map of the difference between the observed and the simulated map. The main feature in the residuals is a localised, unresolved source in the Northern side of the disk, with a peak of 46.1 MJy/sr. This localised source is probably a giant molecular cloud complex - associated with one of the spiral arms, and not considered in the simulated map, which only includes the diffuse component of the model. At this FIR wavelength our model predicts a 11% contribution from the star-forming complexes. The integration of the unresolved source gives a flux density of 9.4 Jy, which is 6% of the total integrated flux density. Furthermore a faint extended source is seen in the southern side of the galaxy, of 4.0 Jy integrated flux density. This makes another 2% of the total integrated emission. Thus the faint localised sources seen in the residual maps are in reasonable agreement with the prediction of our model, which reassures us that the template used in our model and scaled according to our model parameters, SFR and the F factor, are indeed a good representation for the galaxy. Apart from the two sources, a faint extended halo (at  $\sim 1\%$  brightness level) is seen extending at large heights perpendicular to the disk. The interpretation of this halo component is beyond the scope of this paper.

A final comparison can be made between the projected radial profiles of the simulated and observed maps. Due to the larger longitudinal coverage of the ISO data, which embraces the outer, asymmetrical HI disk (Swaters et al. 1997), this time we did not mirror the observed profile. Again, a very good agreement between the model prediction and the observed profiles can be seen in Fig. 6d for the Southern side of the galaxy. The localised FIR source from the northern side of the residual map becomes prominent in the radial profiles as well. There also seems to be an excess of FIR emission at radii larger than  $300''$ , not reproduced by our model. We interpret this result as indicative of a dust disk larger than considered by our model, in which all dust disks are truncated at three scale lengths of the B-band stellar disk. A finer grid of models with varying truncation of the scale length may be needed to reproduce the faint FIR emission at large galactocentric radii.

## 5 The SFRs derived from SED modelling

To statistically evaluate our results for SFR, we compare the SFR characteristics of the 5 edge-on galaxies modelled by us with the larger sample of 61 galaxies with inclinations less than 75 degrees which were studied by Kennicutt (1998) on the basis of  $H_\alpha$  measurements.

Fig. 7 depicts the relation between the disk-averaged surface density in SFR ( $\Sigma_{\text{SFR}}$ ) as a function of the average gas surface density ( $\Sigma_g$ ) for the 5

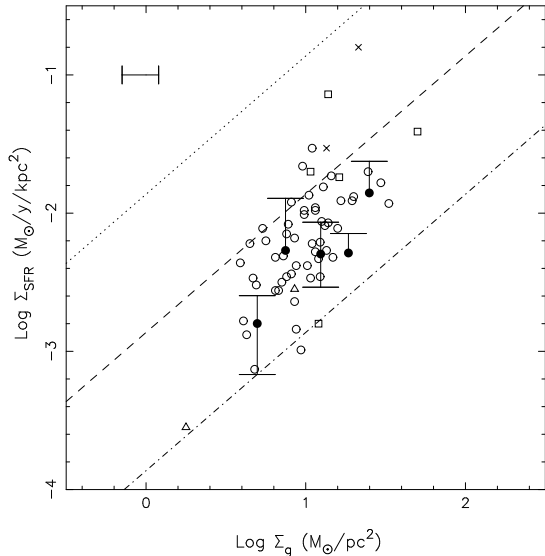


Figure 7: Disk-averaged SFR surface density ( $\Sigma_{\text{SFR}}$ ) as a function of average gas surface density ( $\Sigma_{\text{g}}$ ) for our galaxy sample and for the sample of Kennicutt (1998) of 61 normal disk galaxies with SFR determined from  $\text{H}\alpha$  measurements. The 5 galaxies from our sample are plotted as filled circles and the corresponding  $\Sigma_{\text{SFR}}$ ,  $\Sigma_{\text{SFR}}^{\text{min}}$ ,  $\Sigma_{\text{SFR}}^{\text{max}}$ ,  $\Sigma_{\text{g}}$  and disk areas are listed in Table 3 of Misiriotis et al. (2001). The  $\Sigma_{\text{SFR}}$  are derived from the errors in the IRAS data, e.g. the upper and lower limits for the SFRs are calculated such that the predicted SED is still consistent with the IRAS colours (within the 20% IRAS error bars). The SFR surface densities were calculated by averaging the SFRs over disks with an optically defined boundary ( $R_{\text{o}}$ ) taken to be 3 times the intrinsic radial scalelength  $h_{\text{s}}$  determined from the radiation transfer modelling in the I band. The galaxies from the sample of Kennicutt are plotted as open circles (Sb,Sc,SBb,SBc), triangles (Sa), open squares (Unknown/Not Available), crosses (Irr). The dotted, dashed and dot-dashed lines represent star-formation efficiencies corresponding to consumptions of 100, 10 and 1 percent of the gas mass in  $10^8$  yr.

galaxies. The upper and lower limits for the SFRs are calculated such that the predicted SED is still consistent with the IRAS colours (within the 20% IRAS error bars). Lower error bars are not given when the plotted SFRs represent lower limits for the SFR (maximum values for the factors  $F$ , see discussion in Sect. 3 of Misiriotis et al. 2001). In these cases lower limits would be possible only if we allowed for different sources of uncertainties, like variations in the spectral shape of the template used for the HII regions. However this is hard to quantify, and in the following we assume that the errors of the SFR are given only by the uncertainties in the IRAS data. The plotted data are summarised in Table 3 of Misiriotis et al. (2001) and details

on the calculations of the error bars and of the gas masses can be found in the same paper. The horizontal error bar corresponds to the uncertainty in the gas masses for which we adopted an average 0.2 dex error. The surface area of the disk was calculated for  $R_o = (3 \pm 0.5)h_d$ , where  $h_d$  is the intrinsic radial scalelength determined from the radiation-transfer modelling in the I band. In their analysis of surface photometry of the outer regions of spiral disks, Pohlen et al. (2000) show that the disk boundaries are typically in this range.

The points for the 5 galaxies in Fig. 10 lie within the area of the diagram occupied by the galaxies in the Kennicutt sample. The match is even better for those members of the Kennicutt sample with Hubble types Sb to Sc. This agreement is quite reassuring, bearing in mind the several factors which could introduce a systematic difference between the SFRs inferred for a sample of nearly face-on systems from  $H_\alpha$  measurements compared with the present technique for edge-on systems based on an analysis of broad-band non-ionising UV re-radiated in the FIR-submm range.

Firstly, the  $H_\alpha$  analysis is sensitive to the most massive stars and in particular to the assumed mass cut of  $100 M_\odot$ . Whereas the FIR-submm modelling also assumes the same mass cut in the conversion of SFR to non-ionising luminosity, our model is less sensitive to this effect.

Secondly, whereas the  $H_\alpha$  is sensitive to the star-formation history of the last  $10^7$  yr, our broad-band FIR-submm SED analysis samples approximately the last  $10^8$  yr. Thus, our analysis is consistent with the basic hypothesis (see Kennicutt 1998) for “normal” spiral galaxies of a steady star-formation activity. In principle, we could extend our analysis based on our determinations of the intrinsic populations and use the determined intrinsic colours to determine more accurately the SFR history of the galaxies.

The assumption of a steady-state star-formation rate is also broadly consistent with the timescales for the exhaustion of the current gas supply under the derived SFRs. The dotted, dashed and dot-dashed lines in Fig. 10 represent star-formation efficiencies corresponding to consumptions of 100, 10 and 1 percent of the gas mass in  $10^8$  yr.

Thirdly, the SFRs derived from  $H_\alpha$  were corrected by a single factor for extinction, despite the varying orientations. As well as possibly affecting the vertical position of the galaxies on the plot, this may induce some scatter, especially if all the dust were diffusely distributed. The systematic effect may be expressed in terms of the factor  $F$ : an overestimation of the factor  $F$  is equivalent to an overestimation of the local extinction in the star-formation regions (statistically averaged over the population of HII regions in a disk). Thus, while moving to higher factors  $F$  would move the points for the 5 galaxies towards lower SFRs, it would have the opposite effect for the SFRs determined from the  $H_\alpha$ .

Lastly, we remark that NGC 891 does not appear as an exceptional system compared with the other 4 galaxies in our sample (and with Kennicutt’s [1998] normal galaxy sample) on the basis of SFR normalised to disk area. Our work thus provides no evidence that this galaxy’s exceptional layer of extraplanar

$H_\alpha$ -emitting diffuse ionising gas (e.g. Hoopes et al. 1999) and surrounding X-ray-emitting hot gas (e.g. Bregman & Houck 1997) is attributable to unusual star-formation activity.

## 6 Discussion and Outlook

We have described a “two-dust-disk” model which can successfully account for the observed optical-FIR/submm characteristics of “normal” edge-on spiral galaxies in terms of three fundamental parameters - the  $SFR$ ,  $F$  - the fraction of non-ionising UV absorbed locally in HII regions, and  $M_{\text{dust}}$  - the mass of a second dust disk associated with the young stellar population. We found these parameters to play the key role in determining the amplitude and shape of the FIR-submm SED in galaxies. Some other parameters were given larger attention in the literature, like for example clumpiness, different grain populations, metallicity.

Clumpiness has been extensively discussed by Witt & Gordon (1996, 2000) and used by Gordon et al. (2001) and Matthews & Wood (2001). However, the clumpiness in the interstellar medium is difficult to relate to observations. For example the optical properties of grains in clouds and fundamental parameters such as cloud size and density contrast are poorly known. Because of such uncertainties in the parameterisation of clumpy media, our model does not explicitly incorporate clumps, though our radiative transfer code can treat any arbitrary distribution of emitters and absorbers. However, our model considers implicitly the clumpy distribution in form of the spectral template used for the star-forming complexes. Thus, our model does not include clumps that are not associated with stellar sources, the so called “quiescent clouds”, but does include clouds associated with star-forming regions. As discussed by Popescu et al. (2000), the quiescent clumps must be optically thick to the diffuse UV/optical radiation field in the disk to have an impact on the predicted submm emission. They would then radiate at predominantly longer wavelengths than the diffuse disk emission in the FIR/submm spectral range. One can speculate that such optically thick “quiescent clouds” could be physically identified with partially or wholly collapsed clouds that, for lack of a trigger, have not (yet) begun to form stars. However, due to the lack of intrinsic sources, a very substantial mass of dust would have to be associated with the quiescent clouds to account for a substantial change in the submm SED of galaxies. On the other hand, there may be also dark clouds associated with star-forming complexes. In the Milky Way HII regions around newly born massive stars are commonly seen in juxtaposition to parent molecular clouds (e.g., M17). This is thought to be a consequence of the fragmentation of the clouds due to mechanical energy input from the winds of the massive stars. Thus, warm dust emission from cloud surfaces directly illuminated by massive stars can be seen along a fraction of the lines of sight, together with cold submm dust emission from the interior of the associated optically thick cloud fragments. These dense clumps (with or without asso-



ciated sources) may contribute to the submm emission, and thus supplement the contribution of compact HII regions. Our template for localised sources was successful in reproducing the FIR-submm surface brightness distribution for the prototypical galaxy NGC 891. However, modelling of more galaxies may be needed to check whether our template is a good representation for localised sources, or whether it needs to be supplemented with a submm cold component of dark clouds. More detailed FIR-submm observations of star-forming complexes may also help in improving our HII-region templates.

Different dust populations can produce different types of extinction curves and change the colour of the FIR SED. Our model used the Laor & Draine (1993) silicate/graphite mix, compatible with a Milky Way extinction law. Our choice was based on the agreement between our model extinction curve and the empirical extinction law derived for the studied galaxies independently by Xilouris et al. (1997, 1998, 1999) via the radiative transfer modelling of the optical images. In the case that different galaxies would require different extinction laws, we would adopt a different dust model (chemical composition, grain size distribution).

Finally the metallicity was fixed in our model to be the solar metallicity. Again, this choice was confirmed by the agreement in the extinction curves. A different metallicity may also affect the redistribution of the UV photons with UV wavelengths, as given by the stellar population synthesis models.

In the SED model presented here we did not consider any interactions or effects of inflows/outflows in galaxies. Observationally there is however increased evidence for H $\alpha$  extraplanar emission in galaxies (e.g. Hoopes et al. 1999, Howk & Savage 2000), of X-ray (e.g. Bregman & Houck 1997) and radio halos (e.g. Allen et al. 1978), of galactic (starburst-driven) winds (e.g. Heckman et al. 2000) or for enhanced FIR emission in interacting/merging systems (e.g. Sanders et al. 1998). A discussion of the possible contamination of the FIR disk emission from an extraplanar component has been qualitatively discussed in Popescu et al. (2000b). Moreover, the effect of the cluster environment can also affect the morphology of both stellar and dust distribution, or can produce even more dramatic effects, for example by sweeping the gas and dust material and producing tail-like companions with collisionally heated grains visible in the FIR. As noted by Popescu et al. (2000a), the FIR flux density of the transient IR emission from the dust trail is predicted to rival that of the photon-heated dust in the galactic disk, and, despite the difference in heating mechanism, have similar colours (with a spectral peak in the 100-200  $\mu m$  range). This, combined with removal of dust from the disk, and hence reduced internal extinction, will create a discrete system with brighter apparent blue magnitudes and a boosted spatially integrated IR flux density. If seen in a distant cluster, where the intracluster IR component could not be resolved from the disk component, this could create the illusion of a galaxy with an enhanced star-formation activity, even though the star-formation in the galaxy may actually be somewhat suppressed by the gas removal in reality.

Our model has been applied only to edge-on galaxies, where the scale heights of the old stellar population and old dust disk can be directly deter-

mined. However, our model will also be applicable to face-on systems where the scale heights cannot be so directly determined, making use of UV data as an additional constraint. Although our model requires resolved optical/NIR images to constrain the old stellar population and associated dust, it relies on geometry-sensitive colour information in the FIR/submm to constrain the spatial distributions of young stars and associated dust. The model will therefore be applicable to studies of cosmologically distant “normal” galaxies, which, though detectable, will be unresolved with forthcoming generations of spaceborne FIR observatories. It is to be expected that the optical-FIR-submm SEDs of these objects will differ systematically from their local universe counterparts, not only due to the presence of younger stellar populations, but also, for example, because of evolution of stellar disk thicknesses and changes in the dust abundance and composition.

SED modelling from UV to submm has an important application to interpretation of the cosmological FIR background radiation in terms of constituent galaxies. This particularly applies to the possible contribution from normal galaxies in the early universe, since these are too faint to be observed directly. The development of SED models incorporating a self consistent physical theory for the evolution of these systems may ultimately be needed for this application.

## 7 Acknowledgements

C. Popescu would like to express her gratitude to the organisers of the JENAM 2001 and AG meeting, and especially to Dr. Magdalena Stavinschi, for their invitation to give a Highlight Talk at the meeting. We are grateful to all collaborators in this project, N. Kylafis, A. Misiriotis, J. Fischera and B.F. Madore. We would also like to acknowledge E.M. Xilouris and J. Gallagher for interesting and constructive discussions.

## References

- Allen R.J., Baldwin J.E., Sancisi R., 1978, *A&A* 62, 397
- Alton P. B., Bianchi S., Rand R. J., et al., 1998, *ApJ*, 507, L125
- Alton P. B., Rand R.J., Xilouris E. M., et al., 2000, *A&A*, 356, 795
- Bekki, K., & Shioya, Y. 2000, *ApJ*, 542, 201
- Bianchi, S., Davies, J. I., & Alton, P. B. 2000, *A&A*, 359, 65
- Bregman J.N., & Houck, J. C. 1997, *ApJ*, 485, 159
- Bruzual, A. G., & Charlot, S. 2001, in preparation
- Dale, D. A., Helou, G., Contursi, A., Silbermann, N. A. & Kolhatkar, S. 2001, *ApJ*, 549, 215
- Devriendt, J. E. G., Guiderdoni, B. & Sadat, R. 1999, *A&A*, 350, 381
- Désert, F. X., Boulanger, F., & Puget, J. L. 1990, *A&A*, 237, 215

Draine B. T. & Lee H. M. 1984, ApJ, 285, 89  
 Draine B. T., & Anderson N. 1985, ApJ, 292, 494  
 Dwek E. 1986, ApJ, 302, 363  
 Efstathiou, A., Rowan-Robinson, M., & Siebenmorgen, R., 2000, MNRAS, 313, 375  
 Ferrara, A., Bianchi, S., Cimatti, A., & Giovanardi, C. 1999, ApJS, 123, 437  
 Gordon, K. D., Misselt, K. A., Witt, A. N., & Clayton, G. C. 2001, ApJ, 551, 269  
 Guhathakurta P., & Draine B. T. 1989, ApJ, 345, 230  
 Guélin, M., Zylka, R., Mezger, P. G., et al., 1993, A&A, 279, L37  
 Heckman, T. M., Lehnert, M. D., Strickland, D. K., & Armus, L. 2000, ApJS, 129, 493  
 Hoopes C. G., Walterbos R. A. M., & Rand R. J., 1999, ApJ 522, 669  
 Howk J. C., & Savage, B. D., 2000, AJ, 119, 644  
 Kennicutt, R. C. Jr. 1998, ApJ, 498, 541  
 Kuchinski, L. E., Terndrup, D. M., Gordon, K. D., Witt, A. N. 1998, AJ, 115, 1438  
 Kylafis, N. D., & Bahcall, J. N. 1987, ApJ, 317, 637  
 Laor A., & Draine B. T. 1993, ApJ 402, 441  
 Mathis, J. S., Rumble, W., & Nordsieck, K. H. 1977, ApJ, 217, 425  
 Matthews, L. D., & Wood, K. 2001, ApJ 548, 150  
 Misiriotis A., Kylafis N. D., Papamastorakis J. & Xilouris E. M. 2000, A&A, 353, 117  
 Misiriotis A., Popescu C. C., Tuffs R.J. & Kylafis, D. 2001, A&A, 372, 775  
 Ohta, K. & Kodaira, K. 1995, PASJ, 47, 17  
 Pohlen, M., Dettmar, R.-J., Lutticke, R. 2000, A&A, 357, L1  
 Popescu, C. C., Tuffs, R. J., Fischera, J. & Völk, H. J. 2000a, A&A, 354, 480  
 Popescu, C. C., Misiriotis, A., Kylafis, N. D., Tuffs, R. J. & Fischera, J. 2000b, A&A, 362, 138  
 Popescu, C. C., Madore, B. F., Tuffs, R. J., & Kylafis, N. D. 2001, AAS198, 76.01  
 Popescu, C. C., Tuffs, R. J., Völk, H. J., Pierini, D., & Madore, B. F. 2002, ApJ, 567, 221  
 Sanders, D. B., Soifer, B. T., Elias, J. H., et al., 1998, ApJ, 325, 74  
 Silva, L., Granato, G. L., Bressan, A. & Danese, L., 1998, ApJ, 509, 103  
 Swaters, R.A., Sancisi, R. & van der Hulst, J.M. 1997, ApJ, 491, 140  
 Tuffs, R. J., Popescu, C. C., Pierini, D., Völk, H. J., Hippelein, H., et al., 2002, ApJS, 139, 37  
 Weingartner, J. C., & Draine, B. T. 2001, ApJ, 548, 296  
 Witt, A. N., & Gordon, K. G. 1996, ApJ, 463, 681  
 Witt, A. N., & Gordon, K. G. 2000, ApJ, 528, 799

- Xilouris, E. M., Kylafis, N. D., Papamastorakis, J., Paleologou & E. V., Haerendel, G., 1997, A&A, 325, 135
- Xilouris, E. M., Alton, P. B., Davies, J. I., et al., 1998, A&A, 331, 894
- Xilouris, E. M., Byun, Y. I., Kylafis, N. D., Paleologou, E. V., Papamastorakis, J., 1999, A&A, 344, 868
- Xu, C. & Buat, V., 1995, A&A, 293, L65
- Xu, C. & Helou, G., 1996, ApJ, 456, 163
- Young, J. S., Xie, S., Kenney, J. D. P. & Rice, W. L., 1989, ApJS, 70, 699

**Your title line 1**  
**eventual title line 2**

Author's name  
Institute  
complete address  
email, URL

**Abstract**

*your text of abstract*

**1 Introduction**

text

**2 Part 1**

text

**3 Part 2**

text

**References**

your first reference  
your next reference